agronomy

MDPI

Article

Driving Factors, Regional Differences and Mitigation Strategies for Greenhouse Gas Emissions from China's Agriculture

Shuo Zhou [1], Jianquan Wang [2], Dian Jin [2] and Hailin Zhang [2,*]

[1] College of Science, China Agricultural University, Beijing 100193, China; 2022310030207@cau.edu.cn
[2] College of Agronomy and Biotechnology, China Agricultural University, Beijing 100193, China
* Correspondence: hailin@cau.edu.cn

Abstract

Global warming and climate deterioration are primarily driven by massive greenhouse gas emissions, making the comprehensive assessment of agricultural emissions imperative. This study integrates multiple datasets to achieve three objectives: (1) quantifying agricultural greenhouse gas emissions, (2) identifying regional influencing factors, and (3) exploring mitigation strategies. In this study, a random forest regression model was used to fit the data, providing a new perspective for the analysis of emission factors. Key findings reveal fertilization and irrigation as the dominant emission drivers, with significant regional variations. Specifically, (1) fertilization practices, particularly nitrogen application, exert a greater influence than phosphorus on carbon emissions; (2) irrigation impacts correlate strongly with regional water usage patterns among staple crops; (3) distinct emission patterns emerge across China's northeast–southwest divide, reflecting variations in grain crop impacts and climatic responses. The study proposes three mitigation approaches: precision fertilization, adaptive irrigation management, and crop structure optimization. These strategies provide actionable pathways for China to meet agricultural emission reduction targets while advancing sustainable development goals.

Keywords: climate change; greenhouse gas emissions; agricultural emission drivers; climate-smart agriculture

check for updates

Academic Editor: Jiafa Luo

Received: 30 July 2025
Revised: 19 August 2025
Accepted: 27 August 2025
Published: 28 August 2025

Citation: Zhou, S.; Wang, J.; Jin, D.; Zhang, H. Driving Factors, Regional Differences and Mitigation Strategies for Greenhouse Gas Emissions from China's Agriculture. *Agronomy* **2025**, *15*, 2073. https://doi.org/10.3390/agronomy15092073

Copyright: © 2025 by the authors. Licensee MDPI, Basel, Switzerland. This article is an open access article distributed under the terms and conditions of the Creative Commons Attribution (CC BY) license (https://creativecommons.org/licenses/by/4.0/).

1. Introduction

Greenhouse gases (GHGs) represent one of the primary drivers of global warming and climate change, posing a serious threat to human survival [1–3]. The key contributors to the greenhouse effect—carbon dioxide (CO_2), methane (CH_4), and nitrous oxide (N_2O)—have increased rapidly due to human activities, particularly industrial development and energy consumption [4–6]. Agriculture is a major source of these emissions, responsible for approximately 14% of the global GHG emissions and a significant portion of non-CO_2 emissions (CH_4 and N_2O) [7]. As a significant indicator of the impact of GHGs, the global warming potential (GWP) is notably influenced by the emissions of CO_2, CH_4, and N_2O [8].

The international community has recognized the urgent need to address this challenge. The Paris Agreement sets ambitious targets to limit global temperature increases to well below 2 °C—preferably to 1.5 °C—above pre-industrial levels [9]. Complementing this, the UN General Assembly's call for global carbon neutrality by 2050 adds further impetus for action. Without effective mitigation measures, agricultural GHG emissions are projected to increase by 30% by 2050 [10], highlighting the critical need for intervention.

China's agricultural sector presents a particularly pressing case. As a major agricultural nation, China's farming activities contribute approximately 17% of the country's total GHG emissions, with an average annual growth rate of 5% [11]. This challenge is compounded by China's commitment to achieve carbon neutrality by 2060, while simultaneously needing to meet growing food demands from an expanding population. The dual objectives of enhancing agricultural productivity while reducing emissions create a complex sustainability challenge.

Agricultural emissions are influenced by multiple interacting factors, including the following: physical factors—topography and climate conditions [12]; socioeconomic factors—irrigation practices and farming methods; and regional variations—production conditions and resource endowments. Furthermore, the repercussions of the agricultural sector for human health, freshwater ecotoxicity, and greenhouse gas emissions are attributable to the utilization of fertilizers, pesticides, and herbicides [13–15]. While national-level emission studies exist [16,17], effective mitigation requires localized approaches at the regional or provincial levels [18]. This makes research on provincial disparities in agricultural GHG emissions particularly valuable for policy formulation. Although studies have examined regional variations in countries like Germany, Canada, and Australia [19–21], research focusing specifically on China's provincial differences remains limited.

Recent studies on agricultural GHG emissions [1,22,23] have revealed significant variations across China's provinces in terms of farming practices, climatic conditions, and soil environments. Since China's economic reforms began, the country has achieved remarkable development, reaching its first Lewis turning point by 2004 [24]. However, this rapid progress has also led to regional imbalances, which are reflected in agricultural emission patterns.

Research on spatial variations in agricultural GHG emissions has identified several key influencing factors: regional development levels, the agricultural structure, land use changes, and resource management practices [25,26]. Additional variables that significantly impact emissions include crop types, soil conditions, and temperature effects on soil respiration [27,28]. It has been demonstrated that conventional models are deficient in quantifying the specific magnitudes of the effects of multiple variables. Conversely, the machine learning model adopted in this study has been shown to be capable of numerically demonstrating the significance of the effects of each variable. Current research approaches have certain limitations, e.g., overreliance on traditional models and a lack of interdisciplinary perspectives. They focus on single variables rather than integrated analyses [29,30]. To address these gaps, this study aims to examine region-specific emission patterns through integrated crop–climate modeling, identify systemic drivers using machine learning, and design scalable mitigation strategies for sustainable agriculture.

2. Methods

2.1. Data Sources

The primary data sources for this study include the following:

(1) China's cropping pattern maps (2015–2021) [31];
(2) IPCC greenhouse gas emission datasets [32];
(3) ERA5—the fifth-generation atmospheric reanalysis product from the European Centre for Medium-Range Weather Forecasts (ECMWF) [33];
(4) Fertilizer application rate maps per crop and year [34];
(5) The 2016–2020 National Classification Dataset of Conservation Tillage/Conventional Tillage Farmland [35];
(6) The annual dynamic dataset of high-resolution crop water use in China from 1991 to 2019 [36].

Compared to the frequently used observations from the China Meteorological Administration (CMA), ERA5 demonstrates higher accuracy despite potential minor discrepancies [37]. The dataset spans 2015–2021 and was last accessed on 17 March 2025. Organized by year and region, it covers 30 Chinese provinces, municipalities, and autonomous regions (Figure 1). The time spans for the other datasets are as follows: greenhouse gas emissions dataset: 1970–2022, ERA5: 1950–2025, fertilizer usage map: 1961–2019, cultivation dataset: 2016–2020, water usage dataset: 1991–2019. Based on the existing data range, for model training, we selected data from 2016 to 2019.

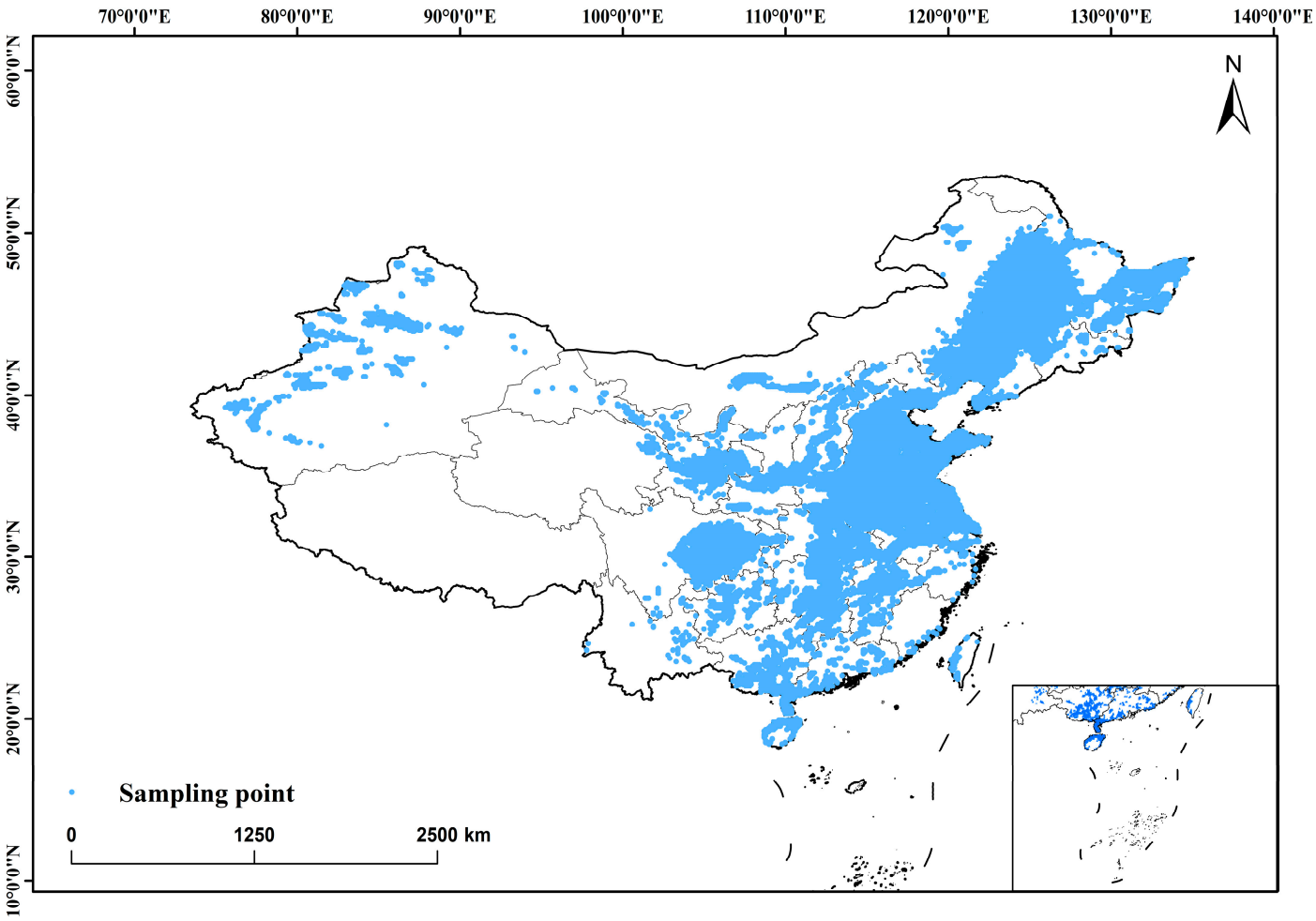


Figure 1. Data sampling points overview. The blue areas indicate the sampling points used in this study.

The independent variables comprise four categories:

1. Ecological zone;
2. Farming practices;
3. Crop type;
4. Climate parameters.

Greenhouse gas emissions—calculated in carbon dioxide equivalents (CO_2-eq)—serve as the dependent variable. This encompasses four components: CH_4, CO_2, N_2O, and the global warming potential (GWP). The GWP metric quantifies the CO_2-equivalent impacts of combined GHGs. The GWP is calculated as follows [38]:

$$GWP(x) = \frac{\int_0^{TH} a_x \cdot [x(t)]dt}{\int_0^{TH} a_\tau \cdot [r(t)]dt}$$

TH is the length of the assessment period during calculation. a_x is the radiative efficiency of one kilogram of gas (unit: W/m^2kg^1). $x(t)$ is the proportion of one kilogram of gas released into the atmosphere at $t = 0$ that decays over time. The numerator is the integral of the chemical substance to be measured and the denominator is the integral of carbon dioxide. As time changes, the radiative efficiencies a_x and a_τ may not remain constant.

The rationale for selecting CH_4, N_2O, and CO_2 greenhouse gas emissions as the dependent variable is that they represent pivotal factors influencing climate change [38]. White et al. have demonstrated that factors such as agricultural practices, crop types, and climate parameters are all important factors affecting greenhouse gas emissions [39].

Factor analyses were conducted individually for all five emission variables. Twenty-two characteristics were included (Table 1).

Table 1. A table of twenty-two characteristics and their corresponding categories.

Category	Characteristic
Ecological zone	Ecological zone
Crop type	Cropclass
Farming practices	Cultivation method
Climate parameters	Tasmax (°C)
Climate parameters	Tasmin (°C)
Climate parameters	Tas (°C)
Climate parameters	Precipitation flux
Climate parameters	Hurs (%)
Climate parameters	Rsds (MJ/m^2)
Farming practices	Maize N (kg/ha)
Farming practices	Maize P_2O_5 (kg/ha)
Farming practices	Maize K_2O (kg/ha)
Farming practices	Wheat N (kg/ha)
Farming practices	Wheat P_2O_5 (kg/ha)
Farming practices	Wheat K_2O (kg/ha)
Farming practices	Rice N (kg/ha)
Farming practices	Rice P_2O_5 (kg/ha)
Farming practices	Rice K_2O (kg/ha)
Farming practices	Maize irrigation
Farming practices	Wheat irrigation
Farming practices	Rice irrigation
Farming practices	Tillage

2.2. Data Processing

In the data processing phase, features were screened using recursive feature elimination (RFE). RFE was initially implemented in the research conducted by Guyon et al. Experiments have demonstrated that genes selected using RFE technology yield superior classification results in comparison to those selected using correlation technology [40]. Subsequent to this seminal work, RFE algorithms have seen widespread application in a variety of feature selection tasks. This method iteratively fits a model using all available features, evaluates their importance, eliminates the least significant ones, and repeats the process until a specified number of features remains. In the RFE algorithm, feature importance reflects the relative significance of predictive factors. Studies have shown that a higher importance value indicates a stronger predictive role of the corresponding factor [41]. The process can be summarized as follows.

1. Initial model fitting: The algorithm fits the model to the complete feature set. Performance metrics—including accuracy, mean squared error (MSE), and other relevant indicators—are recorded.
2. Feature importance ranking: After the initial fitting, features are ranked based on their relative importance. The ranking metrics depend on the selected machine learning algorithm. For tree-based models such as random forests (employed in this study), the Gini impurity or information gain is utilized to determine importance (the present study employs the Gini impurity as a metric).
3. Feature elimination: The least important features are removed from the feature set. This step is critical and requires rigorous execution.
4. Model refitting: The model is refitted using the reduced feature set, and the performance metrics are recorded again.
5. Iteration: Steps 2–4 are repeated until the target number of features is attained or model performance stabilizes.

With regard to the conversion of data, all data utilized in this study remained constant. In instances where discrepancies were observed between sampling points across disparate datasets, the values of the proximate sampling points within 0.1 degrees of the distance delineated in Figure 1 were utilized.

2.3. Model Training

The machine learning model selected as the optimal model for analysis is the random forest regression (RFR) model (Figure 2). Compared to alternative regression models—such as support vector regression (SVR) and multivariate linear regression—RFR demonstrates superior performance due to its algorithmic simplicity, stability, and robust prediction accuracy. The RFR implemented in this study consists of an ensemble of binary decision trees (CART), the principles of CART are detailed in Appendix A. Training the RFR involves training multiple binary decision trees in parallel. During the training of each decision tree, two key considerations are how to select features and how to evaluate their quality. For feature selection, this study adopts an exhaustive method, traversing all previously screened features. To evaluate feature quality, the method is mathematically equivalent to the following proposition:

$$(x, v) = argmin_{x,v} G(x_i, v_{ij})$$

In other words, we find the smallest feature and cut point of G. Here, x_i is a particular cut-off variable, and v_{ij} is a cut-off value of the cut-off variable.

In the random forest regression implemented in this study, Ns denotes the total number of training samples for the current node after splitting. Xleft and Xright represent the training sample sets for the left and right child nodes, respectively.

$$G(x, v) = \frac{1}{N_s}\left(\sum_{y_i \in X_{left}} \left(y_i - \overline{y_{left}}\right)^2 + \sum_{y_j \in X_{right}} \left(y_j - \overline{y_{right}}\right)^2\right)$$

In order to evaluate the carbon emission modeling, the coefficient of determination was used, which is as follows:

$$R^2 = 1 - \frac{\sum_i (y_i - f_i)^2}{\sum_i (y_i - \overline{y})^2}$$

As illustrated in Table 2, the subsequent analysis focuses on the CH_4 emission factors that have been meticulously ranked for Northeast China, subsequent to the training of the models.

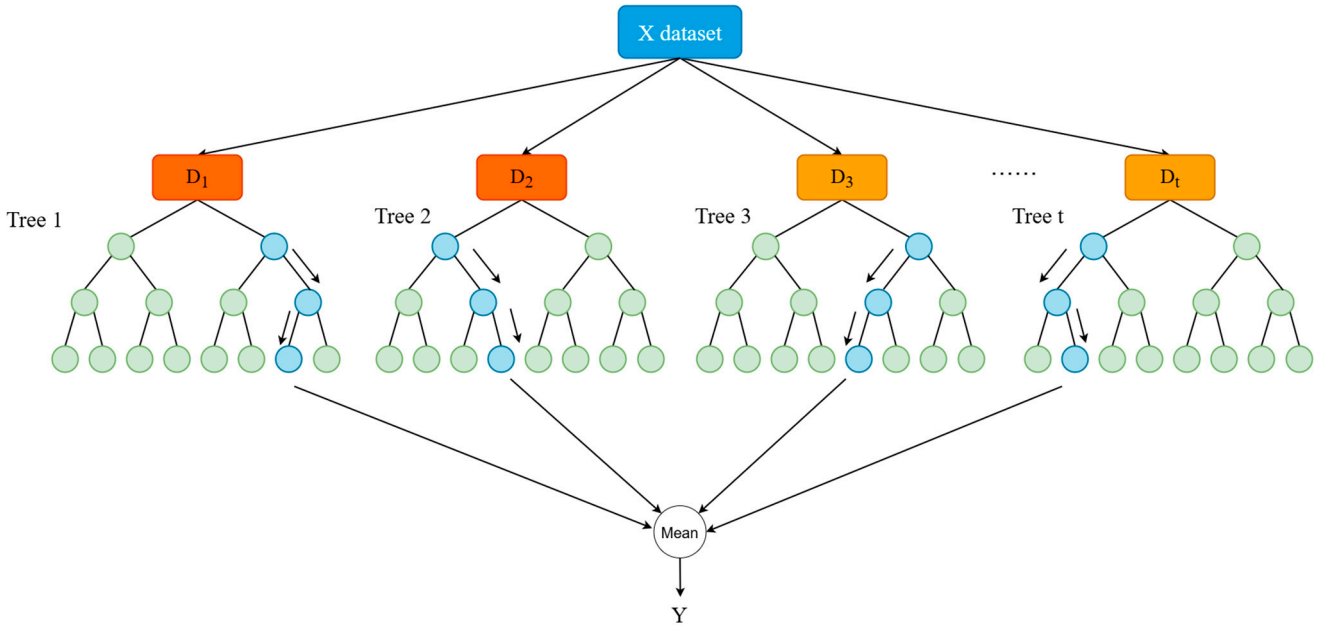


Figure 2. Schematic framework for a random forest regression model. D_1, D_2, D_3, and D_t are all partitions of the dataset X. Tree 1, Tree 2, etc., are CARTs. The blue sections represent branches selected by the tree, while the green sections represent branches not selected.

Table 2. Training results for CH_4 in Northeast China as the dependent variable.

Characteristic	Percentage Importance
Maize irrigation	14.83
Tasmin (°C)	11.59
Wheat irrigation	11.09
Maize N	10.04
Maize P_2O_5	9.70
Wheat N	9.68
Rice irrigation	7.43
Wheat P_2O_5	5.42
Maize K_2O	3.77
Wheat K_2O	3.08
Tas (°C)	2.46
Rice N	1.82
Tasmax (°C)	1.76
Hurs (%)	1.49
Cropclass	1.36
Tillage	1.26
Rsds (MJ/m^2)	0.98
Precipitation flux	0.93
Rice K_2O	0.62
Rice P_2O_5	0.56
Cultivation method	0.14
Ecological zone	0.00

2.4. Geographical Segmentation

In consideration of China's distinct geographical characteristics, the Chinese provinces encompassed within the dataset have been categorized into seven distinct segments. The following regions are located in the Chinese territory: Northeast China, East China, North China, Central China, South China, Southwest China, and Northwest China [42]. The following regions are located in the northeast of China: Heilongjiang, Jilin, and Liaoning.

The eastern region includes Shanghai, Jiangsu, Zhejiang, Anhui, Fujian, Jiangxi, and Shandong. The north of China comprises Beijing, Tianjin, Hebei, Shanxi, and Inner Mongolia. The central region comprises Henan, Hubei, and Hunan; the south includes Guangdong, Guangxi, and Hainan; the southwest encompasses Sichuan, Guizhou, and Chongqing in Yunnan; and the northwest consists of Shaanxi, Gansu, Qinghai, Ningxia, and Xinjiang. The analysis focuses on provinces where the sown area of crops exceeds 4000×10^3 ha, totaling 20 provinces. The 20 provinces include Yunnan, Inner Mongolia, Jilin, Sichuan, Anhui, Shandong, Guangdong, Guangxi, Xinjiang, Jiangsu, Jiangxi, Hebei, Henan, Hubei, Hunan, Gansu, Guizhou, Liaoning, Shaanxi, and Heilongjiang.

3. Results

3.1. GHG Emissions

A comparison of the emissions is depicted in Figure 3, which reveals a general trend of decreasing emissions over time. The following alterations have been observed in the data: CH_4 (−1.28%), CO_2 (−0.90%), GWP (−5.44%), and N_2O (−12.73%). The aforementioned percentages are all negative, thereby indicating that all of the variables are on a downward trend.

3.2. Influencing Factors of Different GHG Emissions

The impact of greenhouse gas emissions is divided into two main categories based on the northeast–southwest divide: the impact on grain crops and the impact on the climate (Figure 4). The impact on grain crops differs between the northern and southern regions: it is more pronounced and relatively weaker in the south.

The northern region is represented by the northwest and northeast. In the northwest, Gansu Province exemplifies the grain crop planting structure, with wheat having the greatest impact. A comprehensive analysis of GWP factors shows that irrigation for corn contributes 12.21% of the impact, with phosphorus fertilizer having the greatest influence on corn fertilization, accounting for 6.71%. Irrigation for wheat accounts for 14.29% of the impact, with nitrogen fertilizer having the greatest influence on wheat fertilization, contributing 13.64%. In terms of CO_2, wheat has the greatest impact among all major grain crops in the northwest, with nitrogen fertilizer having the greatest impact, accounting for 47.29%. In terms of N_2O, corn has the greatest impact among all grain crops in the northwest, with irrigation accounting for 65.76%.

In the northeast region, sampling points are distributed in areas primarily producing corn, which has the greatest impact on greenhouse gas emissions. Regarding GWP, the impact of fertilizers is greater than that of irrigation. The fertilizer with the greatest impact on corn is phosphorus fertilizer, accounting for 24.16%, while irrigation impacts account for 16.01%. Regarding N_2O, the impact of nitrogen fertilizer accounts for 24.57%. Corn has the greatest impact on CO_2, with phosphorus fertilizer having the greatest impact, accounting for 69.77%.

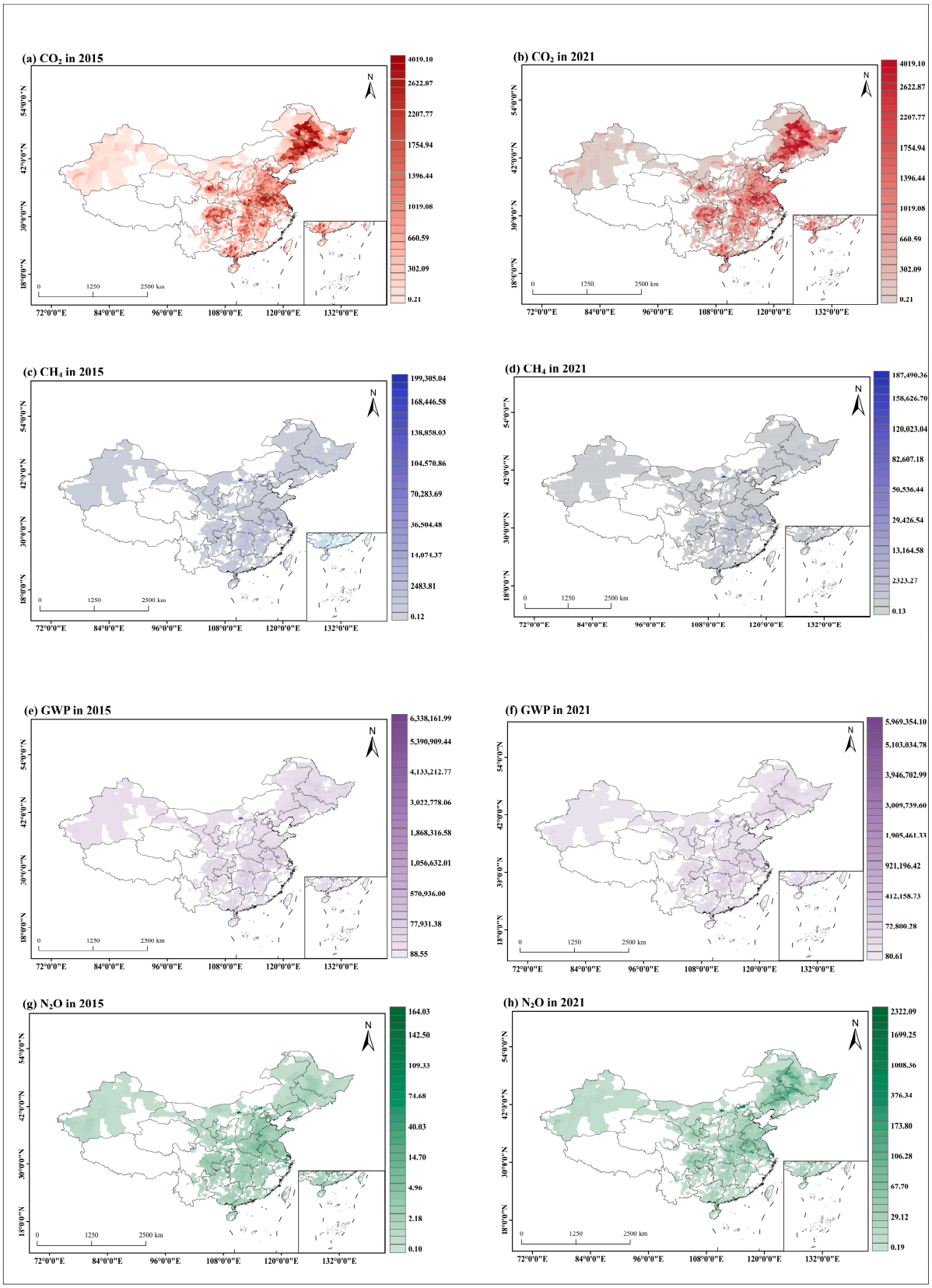


Figure 3. The sum of the GHG emissions from the selected provinces (the data presented on the left are from 2015, while the data on the right are from 2021). (**a**) CO_2 emissions for the year 2015, (**b**) CO_2 emissions in 2021, (**c**) CH_4 emissions in 2015, (**d**) CH_4 emissions in 2021, (**e**) GWP values in 2015, (**f**) GWP values in 2021, (**g**) N_2O emissions in 2015, (**h**) N_2O emissions in 2021.

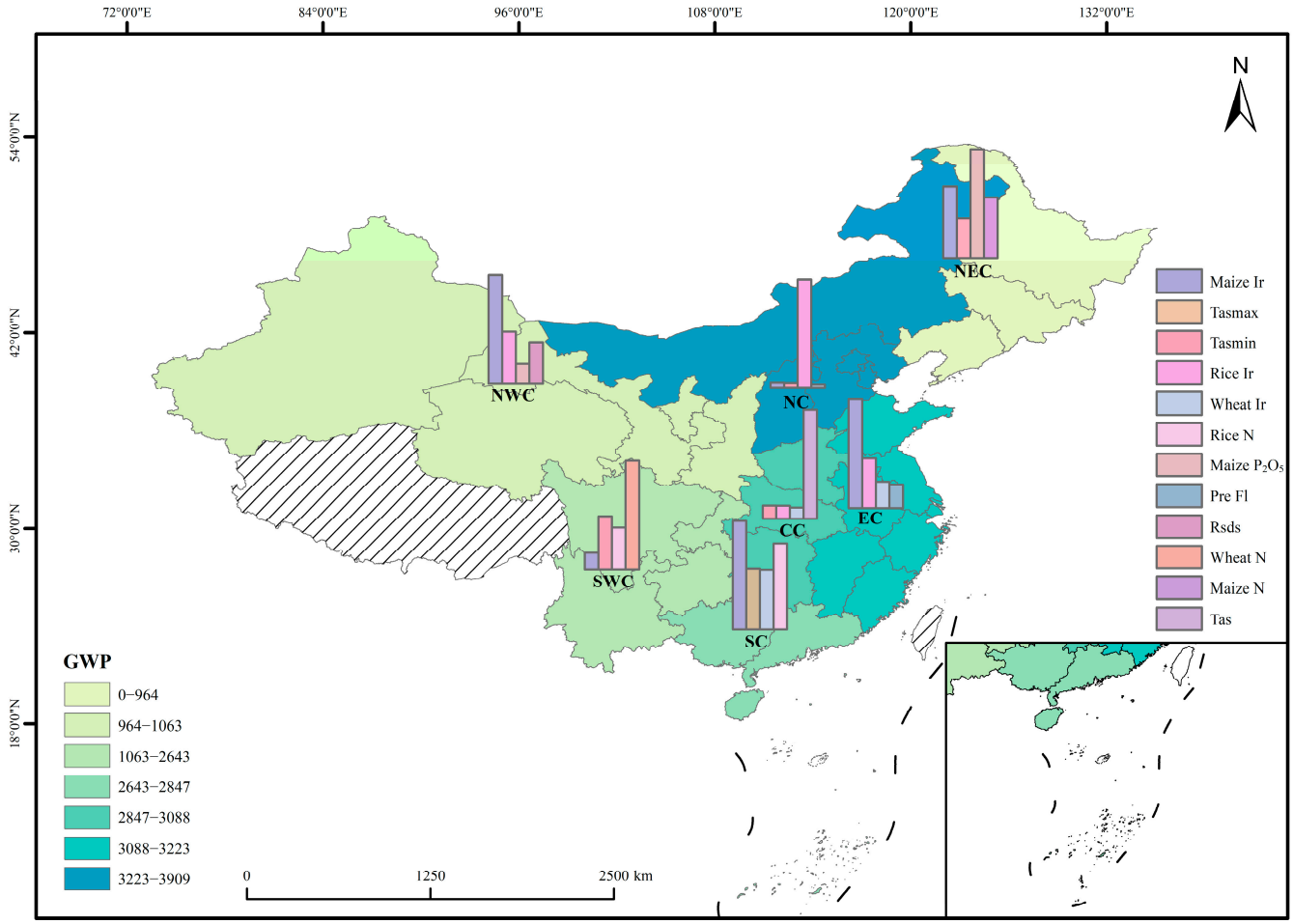


Figure 4. Major regions' GWP and GWP influencing factors. The shaded areas indicate that there are no sampling points in the given province. In the figure, the acronyms "Ir" and "Pre Fl" refer to "irrigation" and "precipitation flux," respectively. The regions of North China, South China, East China, Central China, Northwest China, and Southwest China are denoted by "NC", "SC", "EC", "CC", "NC", and "SWC", respectively.

3.3. Influencing Factors of GHG Emissions in Each Region

The climate impact disparities are distinctly regional. Southern regions below the northeast–southwest divide demonstrate markedly stronger climatic effects than their northern counterparts. This pattern holds across all measured greenhouse gases: for CH_4 emissions, the temperature influence shows dramatic variation—while the maximum temperature accounts for only 0.42% of the impact in North China, it contributes 9.38% in South China. Precipitation effects follow similar regional trends: 0.93% in Northeast China and 0.31% in North China (Figure 5), contrasting sharply with 7.15% in East China and 4.26% in South China. CO_2 impacts reveal comparable geographical patterns. The maximum temperature accounts for 1.12% of the effect in Northwest China but rises to 9.81% in East China (Figure 6). The N_2O data (Figure 7) show precipitation accounting for 0.32% of the impact in North China versus 3.32% in South China. Provincial-level comparisons further emphasize these gradients. The temperature exerts 11.99% of the impact in Guangdong Province, while contributing only 0.33% in Heilongjiang.

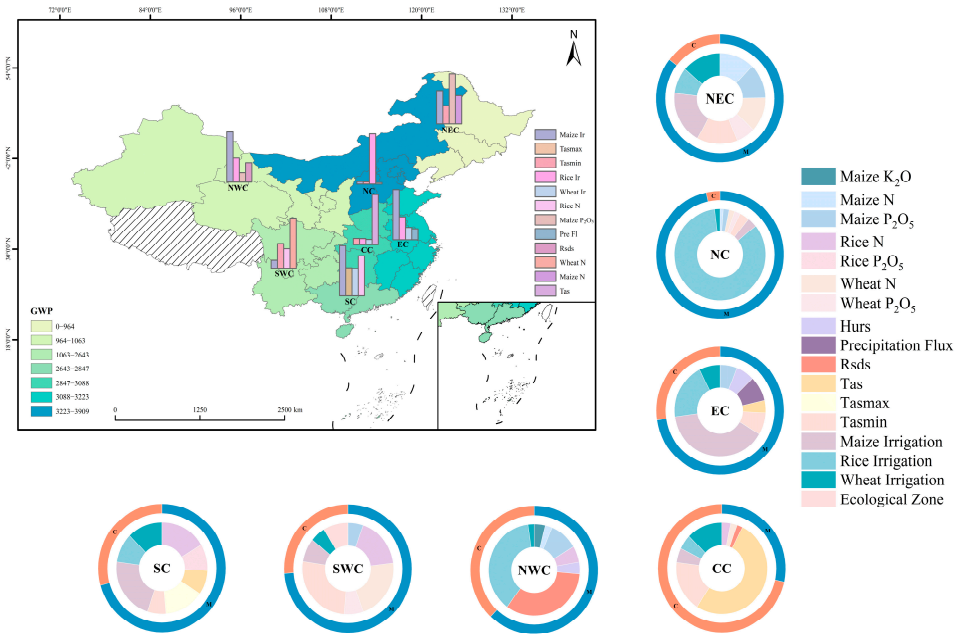


Figure 5. The importance map of CH_4 emission factors derived from the training model for the seven major regions (the circled factors are all eight of the largest percentages). The outer circles of the image, labeled C and M, represent the percentage sum share of the characterizing factors belonging to the climate change category and the percentage sum of the characterizing factors belonging to the agricultural measures category, respectively. In the figure, the regions of North China, South China, East China, Central China, Northwest China, and Southwest China are denoted by "NC", "SC", "EC", "CC", "NC", and "SWC", respectively.

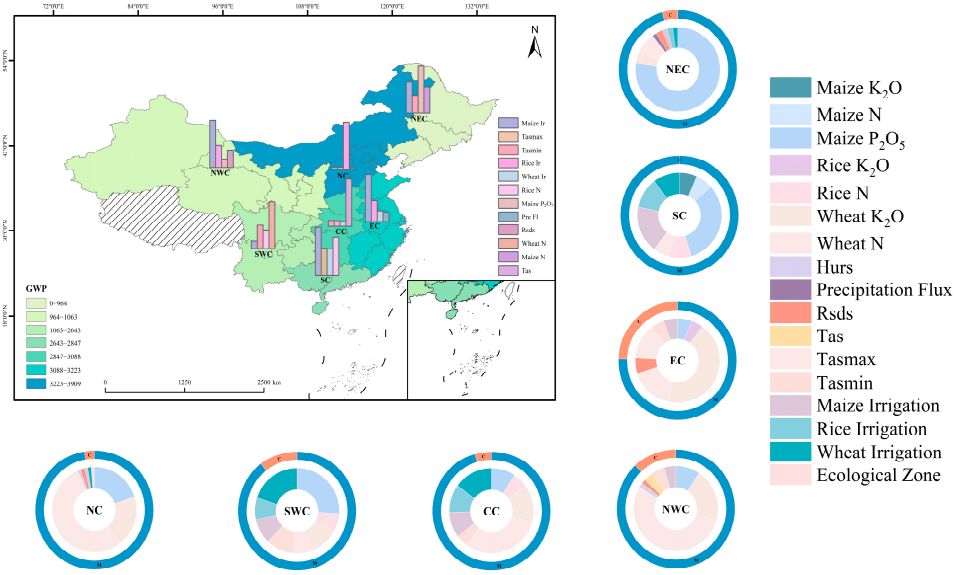


Figure 6. The importance map of CO_2 emission factors derived from the training model for the seven major regions (the circled factors are all eight of the largest percentages). The outer circles of the image, labeled C and M, represent the percentage sum share of the characterizing factors belonging to the climate change category and the percentage sum of the characterizing factors belonging to the agricultural measures category, respectively. In the figure, the regions of North China, South China, East China, Central China, Northwest China, and Southwest China are denoted by "NC", "SC", "EC", "CC", "NC", and "SWC", respectively.

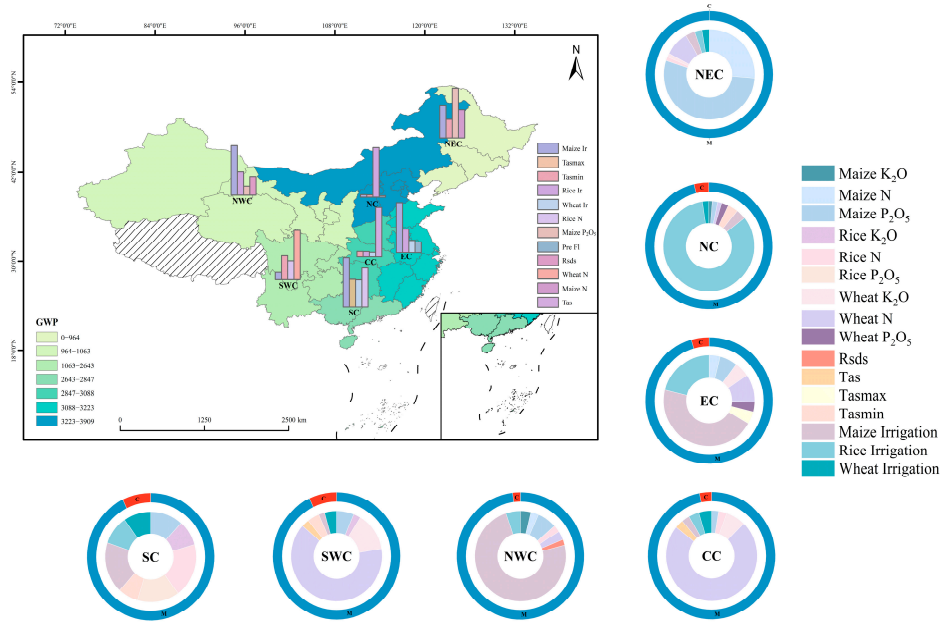


Figure 7. The importance map of N_2O emission factors derived from the training model for the seven major regions (the circled factors are all eight of the largest percentages). The outer circles of the image, labeled C and M, represent the percentage sum share of the characterizing factors belonging to the climate change category and the percentage sum of the characterizing factors belonging to the agricultural measures category, respectively. In the figure, the regions of North China, South China, East China, Central China, Northwest China, and Southwest China are denoted by "NC", "SC", "EC", "CC", "NC", and "SWC", respectively.

4. Discussion

Between 2015 and 2021, China's agricultural carbon emissions exhibited a fluctuating downward trend, with regional differences observed in the primary drivers of emissions. This finding is largely consistent with those in the extant literature on China's agricultural carbon emissions [43]. In contrast to conventional studies, this research applies machine learning algorithms to analyze the variations in drivers across different regions. The objective is to predict the emissions of specific greenhouse gases and identify their respective importance. This study found that fertilizer application and irrigation were the primary drivers of emissions, while significant regional differences were identified between different regions. These findings are consistent with those of previous studies [44,45]. Additionally, the effect sizes of various variables were quantified using a machine learning approach—a methodology that differs from the approaches employed in previous studies. This contributes to establishing a reliable foundation for regional emission reduction measures.

4.1. Recommendations for GHG Emission Reduction

The findings of our research suggest that fertilizers play a significant role in greenhouse gas emissions. Among these, nitrogen and phosphorus fertilizers are pivotal factors affecting carbon emissions, with nitrogen fertilizers typically exerting a more substantial impact than phosphorus fertilizers. A substantial body of research has demonstrated that an increase in fertilizer application rates across various regions and crops results in a notable rise in greenhouse gas emissions [46–48]. To promote environmentally sustainable and low-carbon agricultural development, efforts to reduce fertilizer-related emissions must be strengthened. Achieving this objective requires reducing the excessive use of nitrogen, adopting precision fertilization methodologies, utilizing nitrogen fertilizer enhancers, and applying manure, among other approaches. The efficacy of these methods has been

demonstrated by Tian et al., Cui et al., and Meng et al. [49–51]. It is imperative to acknowledge that emission reduction initiatives must be tailored to the specific conditions of each region. For instance, in the northeast region, a major corn-producing area, the return of crop residues to the field has been demonstrated to reduce fertilizer application. In conventional rice-cultivating regions, such as Jiangxi and Anhui, the practice of rice–crab co-farming can be encouraged to optimize fertilizer usage. Moreover, other nations, such as Thailand, have adopted abatement technologies. These technologies include the utilization of ammonium sulfate in lieu of urea and the implementation of site-based nutrient management. The efficacy of these technologies has been demonstrated in pertinent studies [52].

Another significant factor influencing greenhouse gas emissions is irrigation. Local greenhouse gas emissions are closely related to local crop irrigation volumes. Optimizing low-carbon agricultural production systems offers considerable potential to enhance productivity while mitigating emissions. Numerous studies have proposed methods for mitigating emissions through improved irrigation practices. Wang et al. [53] have indicated that the effective coupling of deficit irrigation and biochar has the potential to reduce crop greenhouse gas emissions while mitigating their negative impacts on crop yields. Yang et al.'s [54] research suggests that, by developing a multiobjective optimization control model, dynamic irrigation control can achieve the synergistic goals of water conservation, emissions reduction, and increased production; moreover, in water-scarce regions, restructuring crop planting patterns is crucial. Some studies estimate that optimizing crop planting structures could reduce the total greenhouse gas emissions from major crops by 10.8%, while also cutting irrigation water use by 13.1%—without compromising national crop production levels [41]. As demonstrated by Yin, Xie, and others [42,43], optimizing crop structures is an effective strategy to reduce the environmental footprint of agriculture. Concomitantly, the alternate wetting and drying (AWD) technique employed in India was determined to be an effective approach to reducing emissions in this nation, as reported by Oo et al. [55].

4.2. GHG Emission Reduction Recommendations for Different Regions

In advancing emission reduction goals, provinces that have achieved significant progress can serve as examples. According to data from the National Bureau of Statistics of China, Anhui has a substantial area dedicated to crop cultivation, with 9044×10^3 hectares of arable land, ranking among the top ten provinces nationwide [38]. Anhui's approach merits particular attention in terms of policy considerations, as evidenced by its noteworthy agricultural scale and emission reduction achievements. As demonstrated in the research by Liu et al., Anhui, a region with a long-standing tradition of rice cultivation, has been undergoing a transformation in its crop structure [56]. This transformation has been characterized by a decline in the cultivation of rice and corn, leading to a notable reduction in emissions. Furthermore, Tong et al.'s research indicates that decoupling grain production from carbon emissions is instrumental in preserving carbon sinks [57]. Consequently, diversifying crop structures emerges as a key strategy for achieving emission reduction targets. It is noteworthy that, from the perspective of carbon emissions in staple food production systems, China's sustainable food system development has achieved significant results, with nearly all agricultural regions demonstrating a trend of increased production and reduced emissions. However, it is important to note that not all regions have the capacity to achieve the balanced development of production and carbon emission reduction in the short term. Optimizing crop structures in line with local conditions, minimizing input consumption, and lowering production costs are essential to achieving meaningful emission reductions.

4.3. Limitations of This Study

While this study offers notable strengths, such as its region-specific driver analysis across multiple emission indicators, several limitations remain for further consideration in future study. A primary consideration is the potential bias in the sampling points of the dataset, which includes instances of null values and missing entries for certain variables. These data gaps may undermine the representativeness of the sample and introduce uncertainty into subsequent analyses. In addition, due to the data limitation, this study did not calculate the biologically derived CO_2 (CO_2bio) emissions, which may lower the actual emissions. Another limitation lies in the scope of the agricultural commodities examined, as the current analysis focuses exclusively on major food crops. This narrow focus overlooks the significant role of fruit and cash crop cultivation in Southern China, where such crops often dominate local agricultural systems. Additionally, discrepancies between real-world field conditions and the emission or climate data integrated into the model could compromise the accuracy of the importance scores derived. Modeled data, by nature, rely on simplifications and assumptions and may not fully capture the complexity of on-the-ground variability—such as microclimatic differences, localized management practices, or temporal fluctuations in emissions. These mismatches have the potential to distort the relative importance assigned to different drivers, thereby affecting the robustness of the conclusions drawn.

4.4. Implications and Policy Recommendations

To achieve the goal of reducing emissions, there is a need for the rationalization of policies, with the overarching objective of reducing emissions in response to this situation. The following recommendations are posited in this study to increase agricultural productivity in order to meet the needs of the growing population, while at the same time reducing greenhouse gas emissions.

This study proposes several recommendations toward these goals. Firstly, policies should be tailored to the specific conditions of each region. For instance, in regions analogous to the 'sickle bend' area of China, cereal yields are low and the ecology is fragile. In other regions, which are generally located in the north, the cultivation of cereals can be reduced and, depending on their location, asparagus or cabbage, which require less sunlight, can be encouraged. Furthermore, the allocation of agri-environmental subsidies for fallow land could be augmented. Within the European Union, farmers who engage in reduced tillage, sustainable agriculture, and precision farming are eligible for subsidies under the Common Agricultural Policy (CAP). The objective of these subsidies is to effectively incentivize farmers to adopt sustainable practices [58,59].

Local governments should promote the adoption of modern agricultural technologies and advancements within their respective regions, with the aim of enhancing the resilience of local agricultural systems in the face of evolving environmental conditions, while concomitantly reducing agricultural greenhouse gas emissions. This approach is instrumental in achieving numerous objectives associated with sustainable development. This concept aligns with the notion of climate-smart agriculture (CSA) systems, a comprehensive approach to agriculture and food production, initially proposed by the Food and Agriculture Organization of the United Nations (FAO) in 2010. As asserted by van Wijk et al. (2020) [60], the utilization of CSA systems is imperative in the reduction of emissions and the mitigation of climate change. Research has demonstrated that the integration of drought-tolerant crop varieties, precision irrigation techniques, and conservation agriculture practices within CSA systems results in substantial productivity gains and a reduction in greenhouse gas emissions [61,62].

Moreover, given the heterogeneity of development across regions, policymakers are able to tailor their responses to specific regional contexts. This may entail the provision of incentives for agriculture or the facilitation of educational and technical opportunities for local farmers, thereby empowering them to adopt environmentally sustainable agricultural technologies. Concurrently, it is imperative to meticulously select and implement farming systems customized to particular locations or soil types to ensure the present generation's ability to meet its needs without compromising the capacity of future generations to do the same [63].

5. Conclusions

This study utilizes a machine learning methodology to examine the correlations between emission indicators and a range of factors in Chinese regions. These factors are predominantly influenced by agricultural practices and climate change. The analysis determined that fertilizer utilization—particularly nitrogen fertilizers—and irrigation are the primary factors influencing greenhouse gas emissions, exhibiting discernible spatial variations. The influence of food crops is predominant in the northern region, delineated by the northeast–southwest line, while it is comparatively negligible in the southern region. In light of these findings, the implementation of diversified emission reduction strategies, such as precision fertilizer application and adaptive irrigation management, is imperative for various regions. Furthermore, the promotion of sustainable agricultural technologies is crucial to achieve the harmonious integration of emission reduction and yield enhancement.

Author Contributions: Conceptualization, S.Z. and H.Z.; methodology, S.Z., J.W., D.J. and H.Z.; software, S.Z.; validation, S.Z. and H.Z.; formal analysis, S.Z.; investigation, H.Z.; resources, S.Z. and H.Z.; data curation, S.Z.; writing—original draft, S.Z.; writing—review and editing, S.Z., J.W., D.J. and H.Z.; visualization, H.Z.; supervision, H.Z.; project administration, H.Z.; funding acquisition, H.Z. All authors have read and agreed to the published version of the manuscript.

Funding: This study was funded by Chinese Universities Scientific Fund (2025TC004).

Data Availability Statement: Agricultural activity data were sourced from the China Crop Pattern Map (2015–2021) at https://figshare.com/articles/dataset/Maps_of_cropping_patterns_in_China_during_2015-2020/14936052 (accessed on 17 March 2025); greenhouse gas emissions data were sourced from the IPCC Greenhouse Gas Emissions Dataset at https://edgar.jrc.ec.europa.eu/dataset_ghg80#p1 (accessed on 17 March 2025); and meteorological data were sourced from the Fifth-Generation Atmospheric Reanalysis product of the European Centre for Medium-Range Weather Forecasts at https://cds.climate.copernicus.eu/datasets/reanalysis-era5-land?tab=overview (accessed on 17 March 2025). The fertilizer data were sourced from fertilizer application rate maps per crop and year at https://figshare.com/articles/dataset/Fertilizer_application_rate_maps_per_crop_and_year/25435432 (accessed on 15 July 2025); the conservation tillage data were sourced from the 2016–2020 National Classification Dataset of Conservation Tillage/Conventional Tillage Farmland at https://cstr.cn/15732.11.nesdc.ecodb.rs.2024.011 (accessed on 15 July 2025); the irrigation data were sourced from data underlying the annual dynamic dataset of high-resolution crop water use in China from 1991 to 2019 at https://doi.org/10.6084/m9.figshare.25980358.v1 (accessed on 15 July 2025).

Acknowledgments: We acknowledge Ruochen Li and Jia Cheng for their assistance in the analysis and express our gratitude to Olatunde Pelumi Oladele for the language polishing.

Conflicts of Interest: The authors declare no conflicts of interest.

Abbreviations

The following abbreviations are used in this manuscript:

GHG	Greenhouse Gas
CO_2	Carbon Dioxide
CH_4	Methane
N_2O	Nitrous Oxide
GWP	Global Warming Potential
IPCC	Intergovernmental Panel on Climate Change
RFE	Recursive Feature Elimination
RFR	Random Forest Regression Model
SVR	Support Vector Regression
ECMWF	European Centre for Medium-Range Weather Forecasts
CMA	China Meteorological Administration
CO_2bio	Carbon Dioxide from Biologically Active Sources
CAP	Common Agricultural Policy
CSA	Climate-Smart Agriculture
Pre Fl	Precipitation Flux
Ir	Irrigation
NEC	Northeast China
NC	North China
SC	South China
EC	East China
CC	Central China
NC	Northwest China
SWC	Southwest China

Appendix A

The Principles of CART

CART is able to obtain the regression tree T by means of the partitioning of the dataset D.

1. Calculate the sum of squared errors for the two parts D_1 and D_2 divided by each feature value and select the optimal feature and optimal split point with the smallest sum of squared errors (as shown in the following equation):

$$\min_{A,a}\left[\min_{c_1}\sum_{x_i\in D_1(A,a)}(y_i-c_1)^2+\min_{c_2}\sum_{x_i\in D_2(A,a)}(y_i-c_2)^2\right]$$

   where c_1 is the mean output of the samples in D_1, and c_2 is the mean output of the samples in D_2.
2. Based on the optimal feature A and the optimal splitting point a, divide the dataset of this node into two parts, D_1 and D_2, and give the corresponding output values:

$$\begin{aligned} D_1(A,a) &= \{x,y\}\in D|A(x)\le a \\ D_2(A,a) &= \{x,y\}\in D|A(x)> a \\ c_1 &= \text{average}(y_i|x_i\in D_1(A,a)) \\ c_2 &= \text{average}(y_i|x_i\in D_2(A,a)) \end{aligned}$$

3. Continue to apply steps 1–2 to the two subsets until the termination condition is met.
4. Generate a regression tree.

When making predictions using the generated CART regression tree, use the mean of the leaf nodes as the predicted output result.

References

1. Ramanathan, V.; Feng, Y. Air pollution, greenhouse gases and climate change: Global and regional perspectives. *Atmos. Environ.* **2009**, *43*, 37–50. [CrossRef]
2. Chamberlain, S.D.; Ingraffea, A.R.; Sparks, J.P. Sourcing methane and carbon dioxide emissions from a small city: Influence of natural gas leakage and combustion. *Environ. Pollut.* **2016**, *218*, 102–110. [CrossRef]
3. Wang, R.; Zhang, Y.; Zou, C. How does agricultural specialization affect carbon emissions in China? *J. Clean. Prod.* **2022**, *370*, 133463. [CrossRef]
4. Lamb, W.F.; Wiedmann, T.; Pongratz, J.; Andrew, R.; Crippa, M.; Olivier, J.G.; Wiedenhofer, D.; Mattioli, G.; Al Khourdajie, A.; House, J. A review of trends and drivers of greenhouse gas emissions by sector from 1990 to 2018. *Environ. Res. Lett.* **2021**, *16*, 073005. [CrossRef]
5. Liobikienė, G.; Butkus, M. Scale, composition, and technique effects through which the economic growth, foreign direct investment, urbanization, and trade affect greenhouse gas emissions. *Renew. Energy* **2019**, *132*, 1310–1322. [CrossRef]
6. Carlson, K.M.; Gerber, J.S.; Mueller, N.D.; Herrero, M.; MacDonald, G.K.; Brauman, K.A.; Havlik, P.; O'Connell, C.S.; Johnson, J.A.; Saatchi, S. Greenhouse gas emissions intensity of global croplands. *Nat. Clim. Change* **2017**, *7*, 63–68. [CrossRef]
7. Beach, R.H.; DeAngelo, B.J.; Rose, S.; Li, C.; Salas, W.; DelGrosso, S.J. Mitigation potential and costs for global agricultural greenhouse gas emissions 1. *Agric. Econ.* **2008**, *38*, 109–115. [CrossRef]
8. Jones, M.W.; Peters, G.P.; Gasser, T.; Andrew, R.M.; Schwingshackl, C.; Gütschow, J.; Houghton, R.A.; Friedlingstein, P.; Pongratz, J.; Le Quéré, C. National contributions to climate change due to historical emissions of carbon dioxide, methane, and nitrous oxide since 1850. *Sci. Data* **2023**, *10*, 155. [CrossRef] [PubMed]
9. Rogelj, J.; Den Elzen, M.; Höhne, N.; Fransen, T.; Fekete, H.; Winkler, H.; Schaeffer, R.; Sha, F.; Riahi, K.; Meinshausen, M. Paris Agreement climate proposals need a boost to keep warming well below 2 °C. *Nature* **2016**, *534*, 631–639. [CrossRef]
10. Tubiello, F.N.; Salvatore, M.; Cóndor Golec, R.D.; Ferrara, A.; Rossi, S.; Biancalani, R.; Federici, S.; Jacobs, H.; Flammini, A. *Agriculture, Forestry and Other Land Use Emissions by Sources and Removals by Sinks*; FAO: Rome, Italy, 2014.
11. He, Y.; Chen, R.; Wu, H.; Xu, J.; Song, Y. Spatial dynamics of agricultural carbon emissions in China and the related driving factors. *Chin. J. Eco-Agric.* **2018**, *26*, 1269–1282.
12. Lepadatu, C. Effects of market reform on agricultural policy community and rural areas. *Sci. Pap.* **2012**, *12*, 105–108.
13. Menegat, S.; Ledo, A.; Tirado, R. Greenhouse gas emissions from global production and use of nitrogen synthetic fertilisers in agriculture. *Sci. Rep.* **2022**, *12*, 14490. [PubMed]
14. Nordborg, M.; Davis, J.; Cederberg, C.; Woodhouse, A. Freshwater ecotoxicity impacts from pesticide use in animal and vegetable foods produced in Sweden. *Sci. Total Environ.* **2017**, *581*, 448–459. [CrossRef]
15. Pathak, V.M.; Verma, V.K.; Rawat, B.S.; Kaur, B.; Babu, N.; Sharma, A.; Dewali, S.; Yadav, M.; Kumari, R.; Singh, S. Current status of pesticide effects on environment, human health and it's eco-friendly management as bioremediation: A comprehensive review. *Front. Microbiol.* **2022**, *13*, 962619. [CrossRef]
16. ACIL Tasman. *Agriculture and GHG Mitigation Policy: Options in Addition to the CPRS*; Report for Victorian Department of Primary Industries and Industry and Investment NSW; ACIL Tasman Pty Ltd.: Melbourne, Australia, 2009.
17. Dace, E.; Blumberga, D. How do 28 European Union Member States perform in agricultural greenhouse gas emissions? It depends on what we look at: Application of the multi-criteria analysis. *Ecol. Indic.* **2016**, *71*, 352–358. [CrossRef]
18. Castesana, P.S.; Vázquez-Amábile, G.; Dawidowski, L.H.; Gómez, D.R. Temporal and spatial variability of nitrous oxide emissions from agriculture in Argentina. *Carbon. Manag.* **2020**, *11*, 251–263. [CrossRef]
19. Brocks, S.; Jungkunst, H.F.; Bareth, G. A regionally disaggregated inventory of nitrous oxide emissions from agricultural soils in Germany–a GIS-based empirical approach. *Erdkunde* **2014**, *68*, 125–144. [CrossRef]
20. Dimitrov, D.D.; Wang, J. Geographic Inventory Framework for estimating spatial pattern of methane and nitrous oxide emissions from agriculture in Alberta, Canada. *Environ. Dev.* **2019**, *32*, 100461. [CrossRef]
21. Musenze, R.S.; Grinham, A.; Werner, U.; Gale, D.; Sturm, K.; Udy, J.; Yuan, Z. Assessing the spatial and temporal variability of diffusive methane and nitrous oxide emissions from subtropical freshwater reservoirs. *Environ. Sci. Technol.* **2014**, *48*, 14499–14507. [CrossRef]
22. Huang, X.; Xu, X.; Wang, Q.; Zhang, L.; Gao, X.; Chen, L. Assessment of agricultural carbon emissions and their spatiotemporal changes in China, 1997–2016. *Int. J. Environ. Res. Public Health* **2019**, *16*, 3105. [CrossRef]
23. Tian, Y.; Zhang, J.; Chen, Q. Distributional dynamic and trend evolution of China's agricultural carbon emissions—An analysis on panel data of 31 provinces from 2002 to 2011. *Chin. J. Popul. Resour. Environ.* **2015**, *13*, 206–214. [CrossRef]
24. Fang, C. China's economic growth prospects: From demographic dividend to reform dividend. In *China's Economic Growth Prospects*; Edward Elgar Publishing: Cheltenham, UK, 2016.
25. Zhang, L.; Pang, J.; Chen, X.; Lu, Z. Carbon emissions, energy consumption and economic growth: Evidence from the agricultural sector of China's main grain-producing areas. *Sci. Total Environ.* **2019**, *665*, 1017–1025. [CrossRef]

26. Tian, Y.; Wu, H. Research on fairness of agricultural carbon emissions in China's major grain producing areas from the perspective of industrial structure. *J. Agrotech. Econ.* **2020**, *1*, 45–55.
27. Koponen, H.T.; Duran, C.E.; Maljanen, M.; Hytönen, J.; Martikainen, P.J. Temperature responses of NO and N_2O emissions from boreal organic soil. *Soil Biol. Biochem.* **2006**, *38*, 1779–1787. [CrossRef]
28. Lu, B.; Song, L.; Zang, S.; Wang, H. Warming promotes soil CO_2 and CH_4 emissions but decreasing moisture inhibits CH_4 emissions in the permafrost peatland of the Great Xing'an Mountains. *Sci. Total Environ.* **2022**, *829*, 154725. [CrossRef]
29. Ullah, A.; Nawaz, A.; Farooq, M.; Siddique, K.H. Agricultural innovation and sustainable development: A case study of rice–wheat cropping systems in South Asia. *Sustainability* **2021**, *13*, 1965. [CrossRef]
30. Shukla, R.; Gleixner, S.; Yalew, A.W.; Schauberger, B.; Sietz, D.; Gornott, C. Dynamic vulnerability of smallholder agricultural systems in the face of climate change for Ethiopia. *Environ. Res. Lett.* **2021**, *16*, 044007. [CrossRef]
31. Qiu, B.; Hu, X.; Chen, C.; Tang, Z.; Yang, P.; Zhu, X.; Yan, C.; Jian, Z. Maps of cropping patterns in China during 2015–2021. *Sci. Data* **2022**, *9*, 479. [CrossRef]
32. Copernicus Climate Change Service (C3S). ERA5-Land Hourly Data from 1950 to Present. Copernicus Climate Change Service (C3S) Climate Data Store (CDS). 2019. Available online: https://cds.climate.copernicus.eu/datasets/reanalysis-era5-land?tab=overview (accessed on 26 August 2025).
33. Coello, F.; Decorte, T.; Janssens, I.; Mortier, S.; Sardans, J.; Peñuelas, J.; Verdonck, T. Global Crop-specific fertilization dataset from 1961–2019. *Sci. Data* **2025**, *12*, 40. [CrossRef]
34. Wang, Y.; Tao, F.; Chen, Y.; Yin, L. Mapping the spatiotemporal patterns of tillage practices across Chinese croplands with Google Earth Engine. *Comput. Electron. Agric.* **2024**, *216*, 108509. [CrossRef]
35. Wang, M.; Shi, W. The annual dynamic dataset of high-resolution crop water use in China from 1991 to 2019. *Sci. Data* **2024**, *11*, 1373. [CrossRef]
36. Jiang, Q.; Li, W.; Fan, Z.; He, X.; Sun, W.; Chen, S.; Wen, J.; Gao, J.; Wang, J. Evaluation of the ERA5 reanalysis precipitation dataset over Chinese Mainland. *J. Hydrol.* **2021**, *595*, 125660. [CrossRef]
37. Griggs, D.J.; Noguer, M. Climate change 2001: The scientific basis. Contribution of working group I to the third assessment report of the inter-governmental panel on climate change. *Weather* **2002**, *57*, 267–269. [CrossRef]
38. Filonchyk, M.; Peterson, M.P.; Zhang, L.; Hurynovich, V.; He, Y. Greenhouse gases emissions and global climate change: Examining the influence of CO_2, CH_4, and N_2O. *Sci. Total Environ.* **2024**, *935*, 173359. [CrossRef]
39. White, J.W.; Hoogenboom, G.; Kimball, B.A.; Wall, G.W. Methodologies for simulating impacts of climate change on crop production. *Field Crops Res.* **2011**, *124*, 357–368. [CrossRef]
40. Guyon, I.; Weston, J.; Barnhill, S.; Vapnik, V. Gene selection for cancer classification using support vector machines. *Mach. Learn.* **2002**, *46*, 389–422. [CrossRef]
41. Khan, N.; Sachindra, D.; Shahid, S.; Ahmed, K.; Shiru, M.S.; Nawaz, N. Prediction of droughts over Pakistan using machine learning algorithms. *Adv. Water Resour.* **2020**, *139*, 103562. [CrossRef]
42. Yang, X.; Yang, Y.; Xu, S.; Karimian, H.; Zhao, Y.; Jin, L.; Xu, Y.; Qi, Y. Unveiling the air pollution tapestry in China: A comprehensive assessment of spatiotemporal variations through geographically and temporally weighted regression. *Atmos. Pollut. Res.* **2024**, *15*, 101987. [CrossRef]
43. Tian, Y.; Yin, M.-H. Re-evaluation of China's agricultural carbon emissions: Basic status, dynamic evolution and spatial spillover effects. *China Rural Econ.* **2022**, *3*, 104–127. (In Chinese)
44. Yang, S.; Chen, H.; Li, Z.; Ruan, Y.; Yang, Q. Temporal and spatial analysis of fertilizer application intensity and its environmental risks in China from 1978 to 2022. *Environ. Sci. Eur.* **2024**, *36*, 188. [CrossRef]
45. Li, C.; Jia, J.; Wu, F.; Zuo, L.; Cui, X. County-level intensity of carbon emissions from crop farming in China during 2000–2019. *Sci. Data* **2024**, *11*, 457. [CrossRef]
46. Shcherbak, I.; Millar, N.; Robertson, G.P. Global metaanalysis of the nonlinear response of soil nitrous oxide (N_2O) emissions to fertilizer nitrogen. *Proc. Natl. Acad. Sci. USA* **2014**, *111*, 9199–9204. [CrossRef]
47. Millar, N.; Urrea, A.; Kahmark, K.; Shcherbak, I.; Robertson, G.P.; Ortiz-Monasterio, I. Nitrous oxide (N_2O) flux responds exponentially to nitrogen fertilizer in irrigated wheat in the Yaqui Valley, Mexico. *Agric. Ecosyst. Environ. Dev.* **2018**, *261*, 125–132. [CrossRef]
48. Yang, L.; Deng, Y.; Wang, X.; Zhang, W.; Shi, X.; Chen, X.; Lakshmanan, P.; Zhang, F. Global direct nitrous oxide emissions from the bioenergy crop sugarcane (*Saccharum* spp. inter-specific hybrids). *Sci. Total Environ.* **2021**, *752*, 141795. [CrossRef]
49. Meng, X.; Liu, S.; Zou, J.; Osborne, B. The effect of substituting inorganic fertilizer with manure on soil N_2O and CH_4 emissions and crop yields: A global meta-analysis. *Field Crops Res.* **2025**, *326*, 109831. [CrossRef]
50. Cui, X.; Chen, S.; Yang, J.; Zhao, L.; Hu, T.; Lu, J.; Li, A.; Zhang, J.; Chang, Z.; Liu, J. Ammonia volatilization and nitrous oxide emission and their responses to environmental indicators under different irrigation levels and nitrogen fertilizer synergists. *J. Environ. Manag.* **2025**, *377*, 124580. [CrossRef]

51. Tian, H.; Xu, R.; Canadell, J.G.; Thompson, R.L.; Winiwarter, W.; Suntharalingam, P.; Davidson, E.A.; Ciais, P.; Jackson, R.B.; Janssens-Maenhout, G. A comprehensive quantification of global nitrous oxide sources and sinks. *Nature* **2020**, *586*, 248–256. [CrossRef] [PubMed]
52. Arunrat, N.; Sereenonchai, S.; Pumijumnong, N. On-Farm evaluation of the potential use of greenhouse gas mitigation techniques for rice cultivation: A case study in Thailand. *Climate* **2018**, *6*, 36. [CrossRef]
53. Wang, T.; Cong, X.; Yu, J.; Zhao, H.; Xu, L.; Pang, G.; Xu, Z. Impact of biochar and deficit irrigation on greenhouse gas emissions reduction in maize-wheat rotation systems. *Agric. Water Manag.* **2025**, *315*, 109547. [CrossRef]
54. Yang, A.; Sun, Z.; Zhang, P.; Hu, K.; Luo, S.; Dong, W.; Li, M. Dynamic Multi-Objective Optimization of Rice Irrigation Integrating Crop Growth and Water Cycle Dynamics: Promoting Synergies in Water Conservation, Production Enhancement, and Emission Reduction. *Environ. Technol. Innov.* **2025**, *39*, 104241. [CrossRef]
55. Oo, A.Z.; Sudo, S.; Inubushi, K.; Chellappan, U.; Yamamoto, A.; Ono, K.; Mano, M.; Hayashida, S.; Koothan, V.; Osawa, T. Mitigation potential and yield-scaled global warming potential of early-season drainage from a rice paddy in Tamil Nadu, India. *Agronomy* **2018**, *8*, 202. [CrossRef]
56. Liu, Z.; Yang, P.; Wu, W.; Li, Z.; You, L. Spatio-temporal changes in Chinese crop patterns over the past three decades. *Acta Geogr. Sin.* **2016**, *71*, 840–851. (In Chinese)
57. Tong, H.; Guo, X.; Shahbaz, M.; Khamdamov, S.-J. Historical carbon emissions and future mitigation potentials from staple food cropping systems in China. *J. Environ. Manag.* **2025**, *389*, 126090. [CrossRef]
58. Grosjean, G.; Fuss, S.; Koch, N.; Bodirsky, B.L.; De Cara, S.; Acworth, W. Options to overcome the barriers to pricing European agricultural emissions. *Clim. Policy* **2018**, *18*, 151–169. [CrossRef]
59. Coderoni, S.; Esposti, R. CAP payments and agricultural GHG emissions in Italy. A Farm-Level assessment. *Sci. Total Environ.* **2018**, *627*, 427–437. [CrossRef]
60. van Wijk, M.T.; Merbold, L.; Hammond, J.; Butterbach-Bahl, K. Improving assessments of the three pillars of climate smart agriculture: Current achievements and ideas for the future. *Front. Sustain. Food Syst.* **2020**, *4*, 558483. [CrossRef]
61. Gerber, P.J.; Steinfeld, H.; Henderson, B.; Mottet, A.; Opio, C.; Dijkman, J.; Falcucci, A.; Tempio, G. *Tackling Climate Change Through Livestock: A Global Assessment of Emissions and Mitigation Opportunities*; FAO: Rome, Italy, 2013.
62. Hellin, J.; Fisher, E. The Achilles heel of climate-smart agriculture. *Nat. Clim. Change* **2019**, *9*, 493–494. [CrossRef]
63. Lal, R. Farming systems for global issues of the 21st Century. *Farming Syst.* **2024**, *2*, 100113. [CrossRef]

Disclaimer/Publisher's Note: The statements, opinions and data contained in all publications are solely those of the individual author(s) and contributor(s) and not of MDPI and/or the editor(s). MDPI and/or the editor(s) disclaim responsibility for any injury to people or property resulting from any ideas, methods, instructions or products referred to in the content.